12B.5 COMPARISON OF DROP SIZE DISTRIBUTION PARAMETER (D_0) AND RAIN RATE FROM S-BAND DUAL-POLARIZED GROUND RADAR, TRMM-PRECIPITATION RADAR (PR) AND COMBINED PR/TMI: TWO EVENTS FROM KWAJALEIN ATOLL

V. N. Bringi[1], Gwo-Jong Huang[1], S. Joseph Munchak[4], Christian D. Kummerow[2]
David A. Marks[3] and David B. Wolff[3]

[1] Department of Electrical and Computer Engineering, Colorado State University, Fort Collins, Colorado
[2] Department of Atmospheric Sciences, Colorado State University, Fort Collins, Colorado
[3] NASA GSFC and Science Systems Applications, Inc., Lanham, Maryland
[4]NASA GSFC and University of Maryland College Park / Earth System Science Interdisciplinary Center

1. INTRODUCTION

Ground validation (GV) of satellite rainfall estimates has been an ongoing component of the Tropical Rainfall Measuring Mission (TRMM) since, and even prior to, its launch in 1997. GV data provide a benchmark for algorithm developers and can be used to tune various assumptions that are required to retrieve rainfall rates from the TRMM instrument measurements. For example, the default coefficients of the Z-R relationship used by the TRMM Precipitation Radar (PR) algorithm 2A25 are derived from disdrometer measurements are a worldwide sampling of locations (Iguchi et al. 2000). GV can also help identify the random, systematic, and sampling errors in rainfall detection and estimation when coupled with the satellite record. When combined with the global constraints on rainfall required by energy budget considerations (e.g., Trenberth et al. 2009), the local constraints provided by GV measurements provide feedback to satellite rainfall algorithm developers enabling them to make estimates that are as accurate and unbiased as possible given the under-constrained nature of the retrieval problem (Stephens and Kummerow 2007).

The large radar and radiometer ground footprints of TRMM necessarily make direct comparisons of instantaneous rain rates from gauges difficult due to the spatial variability of rainfall. Bowman (2005) and DeMoss and Bowman (2007) used 6-hour time centered on each TRMM overpass to match buoy-mounted rain gauge measurements to satellite retrievals. Over long periods of time, systematic biases in the satellite-derived mean rain rate are apparent under this method but large errors exist for individual events.

Corresponding author address: V. N. Bringi, Dept. of Electrical and Computer Engineering, Colorado State University, Fort Collins, CO 80523-1373

E-mail: bringi@engr.colostate.edu

One way to fill the "resolution gap" between the point measurements of gauges and the satellite footprint is through the use of ground-based radars to provide a high-resolution, three-dimensional view of the rain field over a domain larger than the satellite instrument field of view. To achieve this goal, the TRMM GV Program produces quality-controlled ground radar reflectivity fields at 2 km horizontal and 0.5 km vertical resolution using ground radars at Houston, TX (HSTN), Melbourne, FL (MELB), Darwin, Australia (DARW), and Kwajalein Atoll, Republic of Marshall Islands (KWAJ). These products have been used to validate the TRMM measurements in many prior studies. For example, Schumacher and Houze (2000) compared ground-based and PR reflectivities directly at the KWAJ site. This analysis was important in verifying the minimum detectable signal of PR and identifying absolute biases in the reflectivity field, which can lead to rainfall biases.

Studies that compare TRMM GV to satellite-derived rainfall rates are subject to an additional source of uncertainty in the reflectivity-rain rate relationship. Wolff et al. (2005) developed rainfall maps from the KWAJ and MELB radar maps and numerous collocated gauges using the Window Probability Matching Method (WPMM). The WPMM, as used in these studies, aims to reproduce the probability density function (*pdf*) of R (from the gauges) given Z (from the radar) yearly for KWAJ and monthly for MELB. These were compared to TRMM products gridded at 0.5º resolution over a 6-month period, and it was found that PR 2A25 algorithm overestimated rainfall at KWAJ by 6%. Wolff and Fisher (2008) furthered these studies by comparing the WPMM products at the scale of individual TMI and PR footprints over a 5-year period, this time finding that PR 2A25 (2B31) underestimated rainfall by 13% (5.7%) at KWAJ (primarily due to an underestimate of the intensity of heavy rainfall events). Because the WPMM Z-R relationships are re-established each month, seasonal changes in Z-R relationships can be captured, but individual events can still deviate from the monthly mean relationship, which adds a source of variability to the footprint-level comparisons. Because gauges are irregularly distributed over land

and not present over water, it is not possible to tune individual rainfall events to gauge networks due to lack of data.

The potential role of dual-polarization radar in GV of satellite precipitation measurements has been summarized by Chandrasekar et al. (2008). There have been a few studies comparing the DSD parameters from TRMM-PR and ground-based dual-polarized radars. The first such comparison was conducted by Liu et al. (2003) using the CPOL (C-band Polarimetric) radar operated by the then Bureau of Meteorology Research Center (BMRC). They used a variant of the technique developed by Ferreira et al. (2001) to compare D_0 retrieved from Z_{dr} measurements with that inferred from the Version 5 of the 2A25 algorithm (which uses a combination of ε_0 and attenuation-corrected PR-Z_e described by Iguchi et al. 2000). Liu et al. (2003) compared CPOL radar with TRMM overpasses over Darwin (2 "scenes"), SCSMEX (South China Sea Monsoon Experiment; 3) and Sydney (4). On average, they found that over land the D_0 inferred from 2A25 was biased high relative the CPOL-retrieved D_0, whereas over ocean the D_0 agreement was nearly unbiased. However, there was significant scatter of the D_0 on a "pixel" basis. A similar methodology was used by Chandrasekar et al. (2005) where they compared D_0 retrieved from the SPOL (S-band polarimetric) radar with D_0 inferred from 2A25 (Version 5) for one overpass "scene" during the Texas Under Flight Experiment (TEFLUN) and one from the Large Scale Biosphere Atmosphere (LBA) campaign. From a very limited data set, they found that the mean D_0 inferred from 2A25 was biased low relative to SPOL-derived D_0 (normalized bias of around -8%) with fractional standard error of 25%. We note that the method of inferring D_0 from the 2A25 in these studies (i.e., Liu et al. 2003 and Chandrasekar et al. 2005) is very different from that used recently by Kozu et al. (2009).

In this paper we use data from the polarimetric radar (KPOL) on Kwajalein Atoll (described in Section 2) to validate footprint-level estimates of D_0 and rain rate from TRMM-PR (Kozu et al. 2009) and from a combined algorithm (Munchak and Kummerow 2011) that makes use of TRMM-PR and TMI observations. In addition to comparing the rainfall rates in section 3, we place emphasis on the ability of the algorithms to specifically capture characteristics of the raindrop size distribution (DSD) regime at Kwajalein (via the parameter D_0). We discuss these results and compare them to previous studies of DSDs in this region in Section 4, and conclude with a summary in Section 5.

2. DATA SOURCES AND PROCESSING

a. S-band ground radar

The ground radar data used here is from an operational dual-polarized S-band radar located on Kwajalein Atoll in the Republic of the Marshall Islands (the acronym for this radar is "KPOL"). Detailed descriptions of the radar and improved data quality control procedures can be found in Marks et al. (2009; 2011). It is one of the few dual-polarized S-band radars located in an "open" ocean tropical regime and is an invaluable ground validation (GV) site for comparison of rainfall with the TRMM Precipitation Radar (for example, Houze et al. 2004; Wolff et al. 2005).

The key system characteristics and operational modes are described in Marks et al. 2011). Note that dual-polarization capability is based on simultaneous transmission of horizontal (H) and vertical (V) polarizations with equal power, and simultaneous reception of the H and V components of the back-scattered signal via two matched receivers. The nominal system parameters are operating frequency of 2.8 GHz, 3-dB antenna beam width of 1.1°, pulse width of 1.67 μs, PRF of 960 Hz, gate spacing of 200 m, and a total of 779 gates per beam. A number of PPI sweeps (18) at a predetermined set of elevation angles are performed at a rotation rate of 15° s^{-1} and a beam spacing of 1°: this set of PPI sweeps take approximately 10 min to complete. The number of samples available for integration at each resolution volume is 64. The flowchart in Fig. 2 of Marks et al. (2011) describes their quality control algorithm. For each range profile (or, beam), a data mask was generated to separate precipitation from non-precipitation echoes using the standard deviation of differential propagation phase over a 15-gate (or, 3 km) moving window. The classification was based on using a threshold of 12° for the KPOL magnetron-based transmitter system.

Because our goal is to retrieve D_0 from measurement of Z_{dr}, we independently verified for the two events analyzed here (8 September and 26 October, 2008), that the system offset was <0.05 dB (from that deduced by Marks et al. 2011). The measurement fluctuations were reduced to a standard deviation of <0.2 dB using the finite impulse response (FIR) range filter described in Hubbert and Bringi (1995). Accurate calibration of reflectivity (Z_h) is important since we use a composite rain rate retrieval algorithm which uses either of $R(Z_h,Z_{dr})$ or $R(Z_h)$ as described in the next section. We have checked the relative calibration adjustment (RCA) methodology of Silberstein et al. (2008) and Marks et al. (2009) for the two specific TRMM overpass events on 8 September and 26 October 2008. Our "fine-tuning" of the Z_h adjustment for the two events was done using a method based on K_{dp} versus Z_h scatter plots (quantified in terms of contoured frequency of occurrence plots) in rain against scattering simulations using drop size distributions measured by the Joss disdrometer (the latter to be described in the next Section). It was determined that an offset of -2 dB was necessary for the 8 September case, but that an offset of -0.87 dB was determined for the 26 October case (these offsets were independently

confirmed by the self-consistency method described in Section 3c of Marks et al. 2011 applied specifically for these same two days). We are fairly confident that KPOL radar was too "hot" by 2±0.5 dB on 8 September. For the 26 October, our adjustment is within the ±1 dB uncertainty quoted by Marks et al. (2009) for the relative calibration adjustment (RCA; Silberstein et al. 2008).

Fig. 1 shows PPI scan data of measured Z_h on (i) 8 September and, (ii) 26 October 2008 close to the TRMM overpass times. From the reflectivity PPIs, one can infer that the 8 September case was less organized (isolated convection) relative to the more organized convection on 26 October 2008. For case (i), the convection was generally less organized at the overpass time; however a large area of rain with embedded convection occurred a couple hours after the overpass. Case (ii) had larger and more organized areas of rain with embedded convection. On both days, the systems "pushed" into the radar field-of-view from the south and east most likely associated with a wave on the ITCZ (Inter Tropical Convergence Zone). In both cases the height of the 0C level was very near 5 km as determined by soundings for the two days.

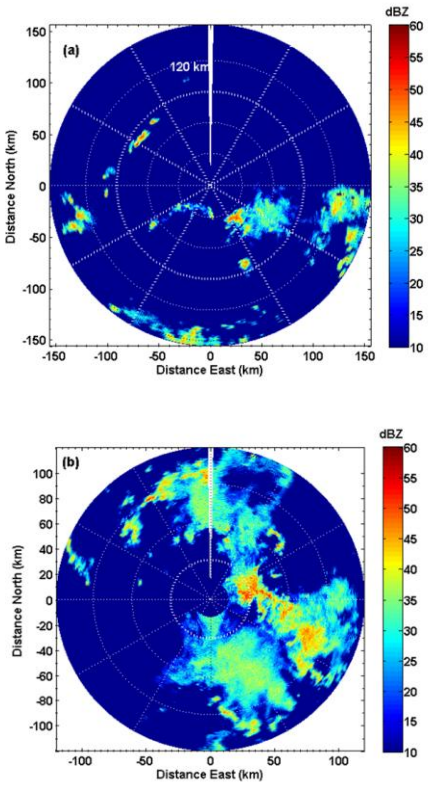

Fig. 1: PPI sweep of reflectivity from KPOL radar at elevation angle of 1.4°, (a) 8 September 2008 during TRMM overpass time, and (b) 26 October 2008.

Fig. 2 shows Z_{dr} versus Z_h from the two events (data from the same corresponding sweeps as in Fig. 1) in terms of contoured frequency of occurrence plots [color scale in *log(number)*]. The dashed line is the mean Z_{dr} in reflectivity bins of 2 dB width. Note that the mean Z_{dr} drops off to a few tenths of a dB (<0.25 dB) as the reflectivity decreases (<15 dBZ) characteristic of nearly spherical drops in drizzle (for example, see Fig. 2 of Brandes et al. 2004). It is interesting to note that in panel (b) corresponding to the more intense organized convection on 26 October 2008, there is a relative lowering of the mean Z_{dr} for Z_h>40 dBZ indicating that at the more intense rain rates, the mean D_0 does not increase with increasing R, rather the increased R is due to increase in drop concentration (for example as discussed in Steiner et al. 2004).

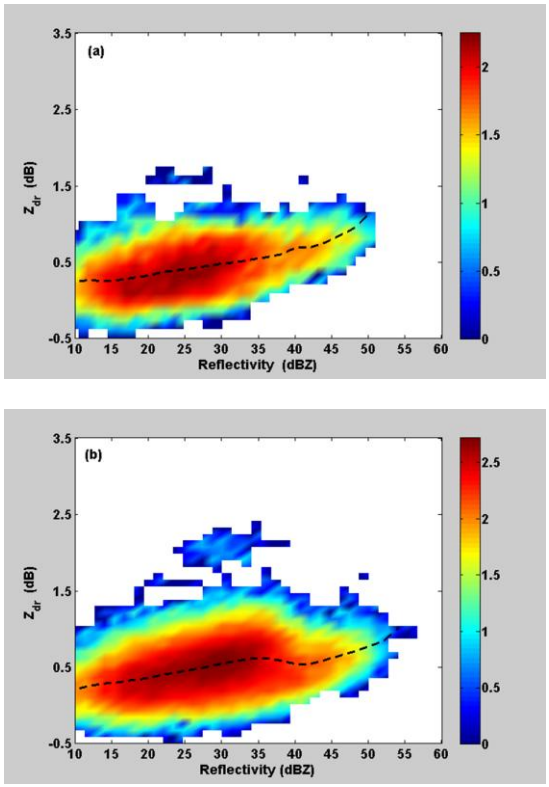

Fig. 2: Contoured frequency of occurrence plots based on scatter plots of Z_{dr} vs Z_h [the color scale is in log(number)] from PPI data from (a) 8 September 2008, and (b) 26 October 26, 2008. The number of "pixels" in panel (a) is

b. Drop size distribution measurements

To develop the D_0 and R retrieval algorithms we use DSD measurements from an impact-type disdrometer (RD-80; Joss and Waldvogel 1967) located at the KPOL radar site. The accuracy of the Joss

disdrometer DSD measurements has been evaluated, for example, by Sheppard and Joe (1994) and by Williams et al. (2000). The disdrometer data were corrected for the "dead time" problem following Sheppard and Joe (1994). Two years of disdrometer data (2003 and 2004) were used in the present study. A total of 69,883 1-minute averaged DSDs were fitted to a normalized gamma distribution with parameters N_w, D_0, and μ, using the procedure given in Bringi et al. (2003). Note that N_w is the "intercept" parameter of the normalized gamma distribution which is the same as the intercept parameter (N_0) of an equivalent exponential DSD with same D_0 and water content, as defined by Illingworth and Blackman (2002) and Testud et al. (2001). Fig. 3 shows the histograms of D_0, $\log_{10}(N_w)$ and μ.

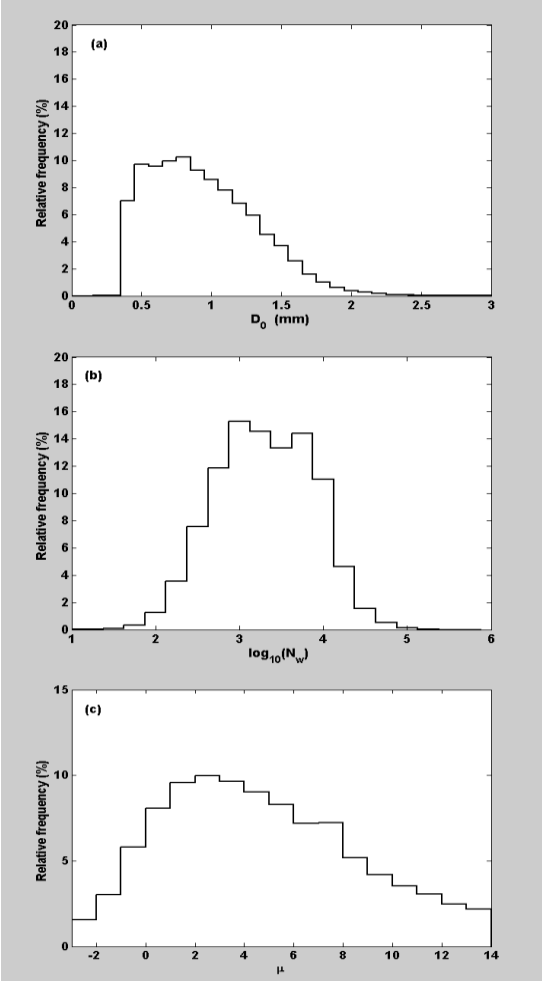

Fig. 3: Histograms of (a) D_0, (b) $\log_{10}(N_w)$ and, (c) μ from Joss disdrometer data from Kwajalein. from (a) 8 September 2008, and (b) 26 October 26, 2008. The number of "pixels" in panel (a) is 15,564 while for panel (b) it is 67,597.

The D_0 histogram shows a modal value close to 0.9 mm but the shape is highly skewed with lower frequency of occurrence of larger Do values relative to the mid-latitudes or the sub-tropics over land (Bringi et al. 2003), perhaps reflecting "open" ocean DSDs (more frequent drop break-up and concentration-controlled DSDs alluded to earlier; Steiner et al. 2004). The histogram of $\log_{10}(N_w)$ is more symmetric with modes at 3000 mm^{-1} m^{-3} (likely stratiform rain mode) and 8000 (perhaps convective rain mode; nearly exactly the same as the intercept parameter N_0 of the Marshall-Palmer exponential DSD). The histogram of μ shows a fairly distinct mode close to 2.5 (we note that Kozu et al. 2009 assume μ=3 which is part of the 2A25 algorithm, Iguchi et al. 2000). The larger values of μ (>8 or so) are likely due to "masking" of the smaller drops in heavier rain (e.g., Williams et al. 2000) or perhaps due to low number of consecutive "bins" in which data occur in light rain (see Fig. 6 of Ulbrich and Atlas 1998).

Scattering calculations using the T-matrix method were performed with the following assumptions: (i) drop shapes based on the most recent 80-m fall bridge experiments [Eq. (1) of Thurai et al. (2007) for D > 1.5 mm and the Beard and Kubesh (1991) fit for 0.7 < D < 1.5 mm, as given in Eq. (3) of Thurai et al. (2007)]; (ii) Gaussian canting angle distribution with mean of 0° and standard deviation of 7.5°, again based on the 80-m fall bridge experiment (Huang et al. 2008); (iii) upper integration diameter of $3.0D_0$ or 8 mm, whichever is less; and (iv) temperature of 20°C and elevation angle of 0°. The T-matrix scattering program outputs, for each fitted DSD (with parameters N_w, D_0, and μ), the values of Z_h, Z_{dr}, and K_{dp}. In this paper we use only the Z_h and Z_{dr} for the retrieval of D_0 and R (the K_{dp} being somewhat noisy except for $\underline{Z_h}$>40 dBZ or so which did not occur often enough in the two TRMM overpass events).

Of importance in this paper, is the retrieval of D_0 from Z_{dr}. From scattering simulations and total weighted least squares method (Amemiya 1997; Lee and Zawadzki 2005) we obtain the D_0 estimator as:

$$D_0 = 1.548\,(Z_{dr}^{0.339}) \quad \text{(mm)};\ Z_{dr} > 0.05\ \text{dB} \qquad (1)$$

The parameterization (or, algorithm) error (see chapter 8 of Bring and Chandrasekar 2001) in the estimate of D_0 in terms of the fractional standard error (FSE) was determined to be 12% (for D_0<2 mm, in agreement with Gorgucci et al. 2002). The FSE of any estimated parameter X is defined as:

$$\mathbf{FSE} = \frac{\sigma_\delta}{\langle R_{disdro} \rangle} \qquad (2)$$

where $\delta = X_{est.} - X_{disdro}$, σ is the standard deviation of δ, and < > denotes the sample mean. Here $X_{est} \equiv D_0$ from (1) and $X_{disdro} \equiv D_0$ from the gamma-fitted DSD. The normalized bias or NB is defined as the mean of δ divided by $<X_{disdro}>$. The NB was found to be negligible (as expected) with reference to the retrieval of D_0. Note that we do not compute D_0 from its definition as the median volume diameter; rather we calculate $D_0 = D_m(3.67+\mu)/(4+\mu)$ where D_m is the mass-weighted mean diameter (ratio of 4^{th} to 3^{rd} moment of the DSD; Ulbrich and Atlas 1998). Since statistical fluctuations in the radar measurement of Z_{dr} cause negative values (see Fig. 2), we empirically retrieve D_0 as:

$$D_0 = 0.355\ Z_{dr} + 0.54 \text{ mm}; \quad -0.25<Z_{dr}<0.05 \text{ dB} \qquad (3)$$

From Fig .2, it is seen that the frequency of occurrence of radar "pixels" with values of $Z_{dr} < 0$ dB is small (<10%). The intercept and slope parameters in (3) have been selected to, (i) merge with (1) at Z_{dr}=0.05 dB and, (ii) tend to the minimum value of D_0 from the disdrometer data (close to 0.45 mm; see Fig. 3a) when Z_{dr} = -0.25 dB. There are other ways to deal with statistical fluctuations of Z_{dr} when retrieving D_0 as described in Bringi et al. (2009). Later when we compare the KPOL-retrieved D_0 with TRMM PR and PR/TMI retrievals, we do so only in convective rain (with rates generally > 3 mm h^{-1}) as determined from the PR.

For rain rate estimation, a simple composite estimator (similar in concept to the synthetic estimator of Ryzhkov et al. 2005) is used based on $R(Z_h,Z_{dr})$ or $R(Z_h)$. For notational simplicity, the subscript 'h' will be dropped, i.e., $Z_h \equiv Z$. The weighted total least squares method was used to derive $Z=302\ R^{1.32}$ and the R(Z) given by:

$$R(Z) = 0.0131\ Z^{0.76} \qquad (4)$$

where Z is in units of $mm^6\ m^{-3}$.

The $R(Z, Z_{dr})$ estimator was based on a non-linear least squares fitting method,

$$R(Z,\ Z_{dr}) = 0.011\ Z^{0.85}\ Z_{dr\ (ratio)}^{-3.28} \qquad (5)$$

where $Z_{dr(ratio)}$ is Z_h/Z_v with $Z_{h,v}$ in units of $mm^6\ m^{-3}$.

Estimator (eq. 5) is used if R(Z) > 10 mm h^{-1} otherwise (eq. 4) is used: this is termed as the composite estimator in this paper. It may be noted, in passing, that the threshold of 10 mm h^{-1} may be used as an approximate classifier between stratiform and convective rain types (e.g., Tokay and Short 1996; Thurai et al. 2010).

The FSE of the parameterization error in the $R(Z, Z_{dr})$ estimator was calculated to be 18.5% with negligible bias. For the R(Z) estimator the corresponding FSE was 67%, in agreement with past simulations (see chapter 8 of Bringi and Chandrasekar 2001 and references contained therein).

c. TRMM-Precipitation Radar

We use Version 6 of the rain profiling algorithm as described in Iguchi et al. (2009). It is not possible to describe this algorithm (referred to as 2A25) in any detail herein because of its complexity. The following variables from the PR are used in this study:

- PR-ZM or the measured reflectivity by the PR (1C21)
- PR-ZC or the attenuation-corrected reflectivity from 2A25 (Iguchi et al. 2009)
- PR-RR or the rain rate from 2A25
- Rain-type flag (here we use only rain classified as "convective" from 2A23; Awaka et al. 2007)
- Attenuation adjustment factor (ε_f) from 2A25

The attenuation adjustment factor for each PR beam is the factor that adjusts the initial coefficient α_0 (in the $k=\alpha_0 Z_e^{\beta}$ relation) such that the Hitschfeld and Bordan (1954) or (H-B) estimate of the path integrated attenuation (PIA) to the surface is equal to the PIA estimated from the surface reference technique (SRT). Kozu et al. (2009) make the inference that the attenuation adjustment factor (henceforth simply referred to as ε) represents to some extent a "path-averaged" DSD parameter. From their Appendix we compute here the D_0 for each resolution volume along the PR slant beam as functions of the 2A25-derived R and ε as:

$$\ln[(D]_0) = \begin{cases} -0.10 + 0.185 * \ln(R) - 1.81 * log_{10}(\epsilon), & \text{convective rain} \\ 0.0976 + 0.1631 * \ln(R) - 1.746 * log_{10}(\epsilon), & \text{stratiform rain} \end{cases} \qquad (6)$$

where R is in mm h^{-1} and D_0 in mm**.**

We use the methodology of Bolen and Chandrasekar (2003) to align the PR measurements with the KPOL ground radar data (the method performs volume matching and geometric distortion corrections). The final product is a gridded Cartesian volume with the ground radar as the origin and with Δx=Δy=4 km and Δz=0.5 km. There are other methods of aligning and volume matching the ground radar reflectivity data with the PR data (e.g., Schwaller and Morris 2011; Wang and Wolff 2009). Fig. 4 shows the horizontal cut of reflectivity at 3 km altitude of attenuation-corrected PR reflectivity (PR-ZC; panel a) and from KPOL (also referred to as GR or ground radar in panel b) for the 8 September case. The spatial alignment of the reflectivity contours is seen to be very good even at such long ranges from ground radar (>130 km). Fig. 5 shows the horizontal cut for the 26 October case (much closer to the ground

radar); again the spatial alignment of the reflectivity contours appears to be very good. Such good alignment sets the stage for comparison of D_0 and R between ground radar and the PR in the rain layer (defined here as heights < 3 km) on a "pixel" basis.

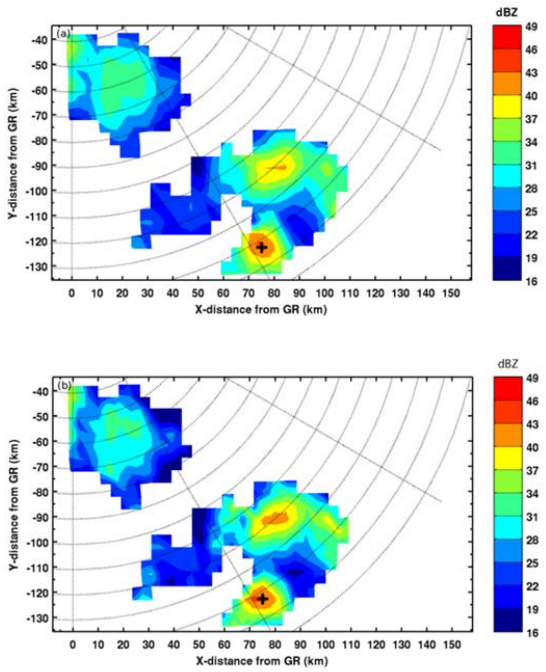

Fig. 4: Constant altitude PPI at 3 km for 8 September overpass, (a) attenuation-corrected PR reflectivity from 2A25, and (b) from KPOL radar. The '+' marks the peak reflectivity.

d. Combined PR/TRMM Microwave Imager

Recently, Munchak and Kummerow (2011), henceforth referred to as MK, have developed and evaluated a combined PR-TMI optimal estimation method of rain profiling which we apply in the present work for the 8 September and 26 October 2008 cases. It is not possible to describe the method here in any detail, except to mention the following points relevant to our paper:

- An optimal estimation technique is used which minimizes a cost function consisting of an observation term and state term.
- The observation term vector consists of the PIA from surface reflection technique and TMI brightness temperatures (which for the low frequency channels, 10, 19 and 37 GHz, are primarily proportional to the total liquid water path).
- The state term vector consists of three parameters which modify the profile-averaged rain DSD, ice PSD, and cloud liquid water content from *a priori* assumptions.
- A radar profiling algorithm similar to 2A25 uses these assumptions together with the measured reflectivity profile ZM to retrieve a hydrometeor profile.
- The cost function, which consists of the weighted departures of observations from forward-modeled values and state parameters from their *a priori* values, is minimized over a large scene to allow convolution of pixel-resolution brightness temperatures to TMI resolution. For this study, the DSD parameters over the entire PR swath intersecting the KPOL coverage area were retrieved simultaneously.
- In the absence of radiometer information, the weighting of the PIA and *a priori* DSD is set to give the same result as 2A25.

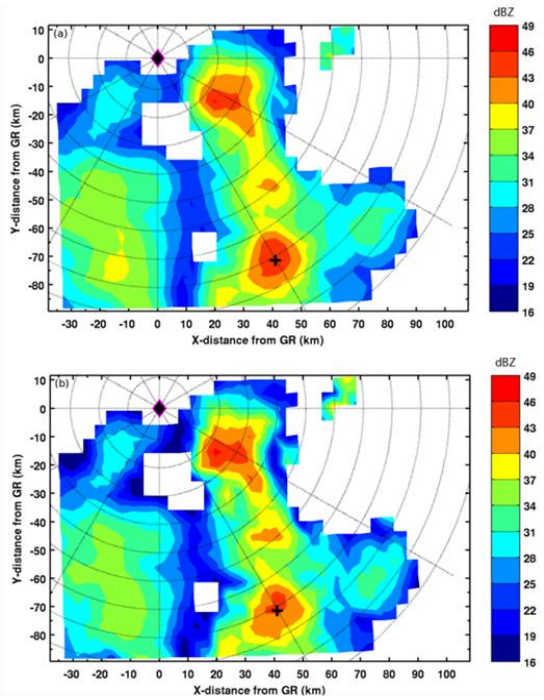

Fig. 5: As in Fig. 4 except for 26 October case

The flow chart in Fig..6 illustrates the modular nature of the overall algorithm. Of relevance here is the D_0 retrieval, which in the MK variational scheme, estimates a parameter ε_{DSD} defined as $D_0=\varepsilon_{DSD}\, aZ^b$, where 'a' and 'b' are *a priori* parameters that have been selected to mimic the default Z-R relationships used by the 2A25 algorithm. This adjustment of the parameter 'a' by ε_{DSD} is similar to the α-adjustment employed by the 2A25 algorithm (Iguchi et al. 2009). The MK algorithm outputs, among other variables, the D_0 and R at each PR resolution volume in the 2A25 format. These data are also aligned and resolution volume matched as mentioned in Section 2c above. Thus, at each grid point of the Cartesian volume we

have available attenuation-corrected Z, D_0 and R from (i) KPOL ground radar, (ii) PR-2A25 algorithm, and (iii) the combined PR-TMI method of MK (both the *a priori* unadjusted values as well as the final retrieved values).

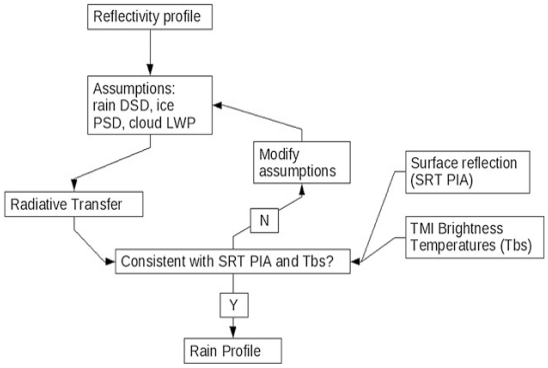

Fig. 6: Flow chart of the combined radar/radiometer estimation scheme adapted from Munchak and Kummerow (2011)

3. KPOL, 2A25 AND COMBINED PR-TMI COMPARISONS

The two TRMM overpass events or "scenes" selected for our analysis are from 8 September and 26 October 2008. Figs. 7-9 show the scatter plots of reflectivity, D_0 and R for the two events. The plots include data from (i) convective rain as flagged by the 2A23 algorithm, and (ii) for heights ≤ 3 km (to ensure that the pixels are well below the 0C level at 5 km). Explanation of the legend is given in Table 1. In each plot the abscissa is data from the KPOL (or, ground radar) and is assumed here to be the ground "truth".

It is important to give an estimate of the retrieval errors, at least on average, for D_0 and R from the KPOL radar so that the scatter (in Figs. 7-9) can be placed in some context. The total error of the KPOL-retrieved D_0 or R is the sum of the parameterization and the measurement errors, expressed as variances (e.g., chapter 8 of Bringi and Chandrasekar 2001). The standard deviation of the measurement of Z_{dr} (from the radar data) was estimated to be 0.2 dB after FIR filtering in range. For Z_h, we assumed the standard deviation to be 1 dB. The FSE of the measurement error in D_0 (due to measurement error in Z_{dr}) is estimated from (1) as 12% at a single radar resolution volume. Because of spatial averaging over the 4X4 km pixel, we estimate that the FSE will be further reduced to < 3%. Hence, the error in the D_0 estimate will be dominated by the parameterization

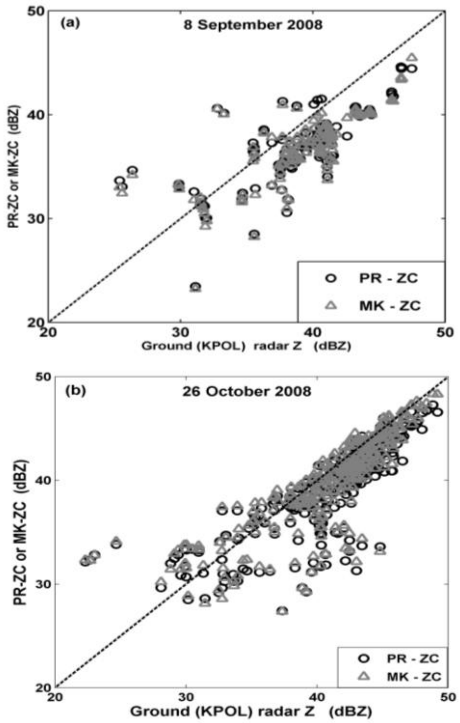

Fig. 7: Scatterplot of reflectivity from (a) 8 September and, (b) 26 October 2008 events.

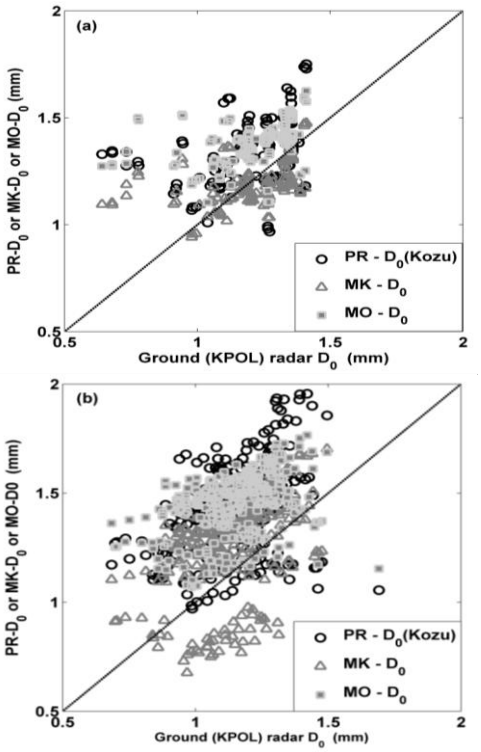

Fig. 8: As is Fig. 7 except scatterplot of D_0

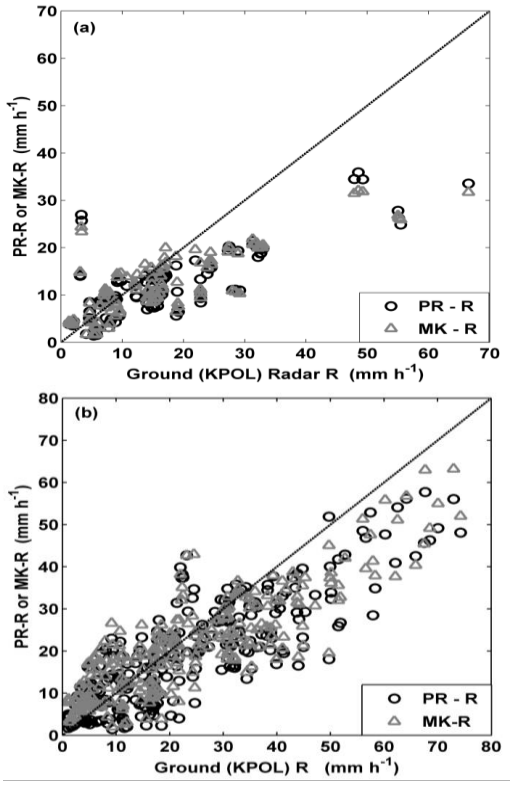

Fig. 9: As in Fig. 7 except scatterplot of R

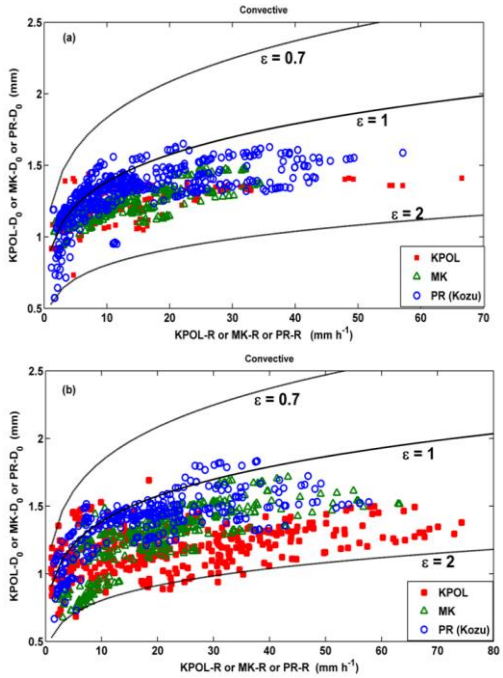

Fig. 10: D_0 versus R scatterplot with contours of constant ε for, (a) 8 September and, (b) 26 October events

Table 1: Legend for Figs. 7-10

PR-ZC	Attenuation-corrected reflectivity from PR
MK-ZC	Attenuation-corrected reflectivity from Munchak and Kummerow (2011) combined PR-TMI methodology (MK)
MO-D_0	Unadjusted D_0 from MK scheme
MK-D_0	Final D_0 retrieved from MK scheme
PR-D_0 (Kozu)	D_0 calculated from eq 7 (from Kozu et al. 2009)

Table 2: Statistics for the 08 September 2008 case (negative bias here means that the respective algorithm used under estimates the KPOL radar estimates and vice versa)

Parameter	Algorithm used	FSE (%)	Normalized bias (%)
D_0	PR-D_0 (Kozu)	16.0	11.7
	MO-D_0	13.4	15.1
	MK-D_0	12.9	-0.8
R	PR-R	49.5	-28.5
	MK-R	50.2	-24.6
Reflectivity	PR-ZC	7.8	-5.3
	MK-ZC	7.5	-5.5

error (the corresponding FSE was 12% as discussed in Section 2b). Similarly, for the R(Z,Z_{dr}) estimate, the FSE due to measurement error (after spatial averaging) Is estimated at 6.4%. Hence, again the error in the estimate of R(Z,Zdr) will be dominated by the parameterization error (the corresponding FSE was 18.5% as discussed in Section 2b). The retrieval errors for D_0 and R from the 2A25 algorithm and from the combined PR/TMI method of MK are not estimated here due to the complexity of the respective

algorithms and given that we are comparing just two "instantaneous scenes" from the TRMM overpasses.

Table 3: As in Table 2 except for the 26 October 2008 case

Parameter	Algorithm used	FSE (%)	Normalized bias (%)
D_0 (mm)	PR-D_0 (Kozu)	18.2	24.6
	MO-D_0	15.0	26.1
	MK-D_0	19.0	9.7
R (mm h^{-1})	PR-R	40.0	-16.2
	MK-R	38.3	-10.9
Reflectivity (dBZ)	PR-ZC	8.6	-3.3
	MK-ZC	8.6	-2.2

Table 2 summarizes the FSE and normalized bias (NB) for the 8 September 2008 case and similarly Table 3 summarizes for the 26 October case. Form the two cases the following points can be noted:

- The correlation between PR-ZC or MK-ZC and the KPOL-Z is high for both events mainly for Z>40 dBZ (Fig.7) as also evidenced by the low FSE in Tables.1 and 2. However, a significant bias (underestimate) can be noted in the PR-ZC and MK-ZC relative to KPOL-Z (around -2.5 dB for 8 September and -1.5 dB for 26 October cases). Recall that for these two specific days, the KPOL-Z was adjusted downwards by 2 dB (for 8 September) and 0.87 dB (for 26 October) relative to the RCA (Silberstein et al. 2008; Marks et al. 2009). To remove the bias in Fig. 7, we would have to further adjust KPOL-Z downwards by 2.5 dB (for 8 September) and 1.5 dB (for 26 October) which is unreasonable (Marks et al. 2009). The conclusion is that the PR-ZC or MK-ZC algorithms have not been sufficiently corrected for attenuation perhaps due to underestimation of the path integrated attenuation (or PIA) from the surface reference technique (SRT). This systematic underestimate of PR- and MK-ZC could be a consequence of non-uniform beam filling effects, which always lead to an underestimate of Z (but not necessarily R) if a uniform beam is assumed (Iguchi et al. 2009), as in the MK algorithm and 2A25- V6.

- The FSE of PR-D_0 or MK-D_0 is of the same order as the FSE of the parameterization error of the KPOL-retrieved D_0.

- The normalized bias of PR-D_0 and the unadjusted MO-D_0 are such that they systematically overestimate the KPOL-retrieved D_0 by 11-15% for the 8 September case and by 24-26% for the 26 October case.

- Most importantly, the bias in MK-D_0 (final retrieval from combined PR/TMI) is reduced substantially to -0.8% for the 8 September case and 9.7% for the 26 October case; this bias reduction likely implies that the TMI data have been valuable in adjusting the final MK-D_0 in the "correct" direction assuming that the KPOL-D_0 is the ground "truth".

- The FSE of rain rate (PR-R and MK-R) is much larger than the FSE of the parameterization error for R from the KPOL radar (18.5%); perhaps some portion of the scatter in Figs. 9 may be ascribed to the fact that the KPOL sample volume-averaged D_0 or R cannot represent the PR sample volume-averaged equivalents (sometimes referred to as "representativeness" error as in Ciach and Krajewski 1999).

- Even though the correlation between the rain rates is high, there is substantial bias (underestimate) of both PR-R and MK-R relative to KPOL-retrieved R (-24 to -28% for 8 September) and less so (-10 to -16% for 26 October). In the case of PR-R, as noted earlier the PR-D_0 is overestimated and thus the corresponding rain rate will generally be underestimated (for a given reflectivity); in addition, the PR-ZC itself underestimates the KPOL-Z by 2.5 dB for 8 September and 1.5 dB for 26 October (Fig. 7a,b). Both factors contribute to the negative bias in PR-R. The fact that MK-R and PR-ZC are biased low relative to KPOL even while MK-D_0 is unbiased can only be reconciled if the cloud water content assumed by the MK algorithm is reduced. This would allow for larger reflectivity to produce the same total (rain plus cloud) water content with the same D_0 and higher R. Of course the caveat is that the KPOL-R is *a priori* assumed to be the ground "truth".

Finally, in Fig. 10 we show scatter plots of D_0 versus R from KPOL radar, from PR (Kozu) and MK algorithms for, (a) 8 September and (b) 26 October cases. Superimposed are lines of constant ε (0.7, 1 and 2) from (6). Most of the convective rain (as flagged by the PR) data fall in the region where $1<\varepsilon<2$, typical in general for "open" ocean rainfall; however, the statistics of ε over the ocean from Kozu et al. (2009) shows the values to be more symmetrically distributed about 1 (with standard deviation of 0.3). Whereas Kozu et al. (2009) relate changes in ε to the multiplicative coefficient 'a' in the $Z=aR^b$ relation, we choose to, equivalently, relate it to a more physical parameter of the DSD such as the median volume diameter (D_0). For example, for a given rain rate, larger values of ε in Kozu et al. (2009) would be interpreted as a smaller value of the coefficient 'a', or smaller D_0 herein. In Fig. 10a, on average for R>5 mm h^{-1}, the KPOL and MK data points fall along a contour of larger ε (relative to the PR data points). This corresponds to an average downward shift of D_0 or the coefficient 'a'. For the higher R>30 mm h^{-1}, the D_0 values tend to lie in a narrow interval (nearly independent of R) corresponding to concentration-controlled DSDs or to equilibrium-like DSDs (Hu and Srivastava 1995). In Fig. 10b, on average for R<30 mm h^{-1}, the MK data tend to lie along a contour of larger ε relative to PR whereas for R>30 mm h^{-1}, not much difference in the average ε between MK and PR data points can be seen. However, for the KPOL data points there is a significant increase in average ε relative to PR or MK for R>20 mm h^{-1} (i.e., lower average D_0 or coefficient 'a' inferred from KPOL relative to MK or PR).

4. DISCUSSION OF RESULTS AND COMPARISON WITH RELATED WORK

The results presented in Section 3 must be understood in the context of the assumptions required by the algorithms used to retrieve D_0 and R from PR reflectivity measurements and, in the case of the MK algorithm, TMI radiances. The PR-2A25 algorithm uses default Z-R relationships for stratiform and convective rain that are only adjusted when the apparent decrease in surface reflection exceeds its normal variability under clear-sky conditions. This variability is typically 1-2 dB which prevents useful adjustments to ε from being made at rain rates less than about 10 mm h^{-1} (Meneghini and Jones 2011). This can be observed in Figure 10, where it can be seen that most of the PR points appear to follow the $\varepsilon=1$ curve, especially below 10 mm h^{-1}. An important assumption in the 2A25 algorithm is that ε is invariant with range along a given beam. Thus, even if the SRT PIA is being correctly matched, the D_0 at a given level may be incorrect.

Many of these same assumptions apply to the MK algorithm as well, except that the radiometer brightness temperatures are used to adjust the DSD both with and in the absence of a reliable SRT PIA value. As a result, at the heaviest rain rates the PR 2A25 and MK methods match up fairly well in terms of retrieved D_0. It is at the lighter rainfall rates where the PIA is not as reliable that the radiometer adjustment becomes important and causes the results to deviate from 2A25. In the two cases presented here, a robust result is that the positive bias in D_0 from 2A25 (relative to KPOL-D_0) is "removed" from using the MK algorithm independent of the rain rate.

Another assumption in both algorithms is the partitioning of rain and cloud water. Cloud water does not significantly affect attenuation at 13.8 GHz relative to rain, so this is thought to be a minor issue for PR 2A25 (Iguchi et al., 2009). However, it has a more significant impact on higher-frequency brightness temperatures, and the partitioning (specifically, the uncertainty in the *a priori* cloud water profile) was set in Munchak and Kummerow (2011) so that the combined algorithm matched the KWAJ rainfall rate over a 6-month period. Even though this partitioning should be correct in the long-term mean, there may be substantial deviations in individual events (see 6th bullet in Section 3). Both 2A25 and the MK algorithm assume a gamma distribution with $\mu=3$. Deviations from this assumption may result in incorrect D_0 values, but R is expected to be more stable as both the PIA and brightness temperatures are responsive to liquid water content, which is closely tied to R. Finally, an error source in the MK algorithm not present for 2A25 is the larger size of the radiometer footprint (10-60 km, depending on frequency) relative to the PR pixel size (4 km). Thus, some of the information used to adjust the D_0 from its default value may be "smoothed" relative to the fine resolution of PR and KPOL.

Regardless of the algorithm used, the bulk of rainfall in these two cases appears to have smaller D_0 and higher R than are expected from the default 2A25 relationships at a given reflectivity. None of the assumptions in either algorithm can change the direction of this adjustment, only its magnitude; thus, we consider it a robust result.

The tendency found here towards higher R and lower D_0 than 2A25 is consistent with the TRMM combined product (2B31; Haddad et al. 1997), which was found to adjust rainfall at KWAJ by 7% over 2A25 by Wolff and Fisher (2008). Grecu et al. (2004), using an experimental combined PR-TMI algorithm, tended to increase N_0* (same as N_W; Testud et al. 2001) at KWAJ, implying DSDs with smaller median drop sizes and larger rain rates than retrieved by the 2A25 algorithm. However, their algorithm increased bulk rainfall by 28% over 2A25, which is greater than biases identified by Wolff et al (2005) and Wolff and Fisher (2008). Note that Munchak and Kummerow (2011) were able to match KWAJ rainfall by including the cloud water adjustment in their optimal estimation

scheme. Comparing their results over KWAJ and MELB (Melbourne, FL) to disdrometer data, Munchak and Kummerow (2011) found that while their retrieved D_0 values were smaller than the disdrometer observations at both sites, the separation of D_0 values between sites was consistent with the disdrometer-measured separation, pointing to either a systematic overestimation of D_0 by the disdrometer or underestimation of D_0 by the combined algorithm. The results presented in this study suggest the former may be correct, given that KPOL- and MK-derived D_0 match quite well in a bulk sense and also exemplifies the additional DSD information present in combined radar-radiometer retrievals since different DSD properties were retrieved at MELB without modification of any algorithm assumptions.

5. SUMMARY

Two TRMM-overpass events or "scenes" over Kwajalein are used to compare KPOL ground radar data with Version 6 of the 2A25 algorithm (Kozu et al. 2009) and a combined PR-TMI algorithm of Munchak and Kummerow (2011). The original contribution of this work is the retrieval of the median volume diameter (D_0) from KPOL-measured Z_{dr} which are then compared with the corresponding retrieval of D_0 using Kozu et al. (2009) via the parameters ε and R from 2A25. In addition, the retrieval of D_0 (and its adjustment from the *a priori* values) using a combined PR-TMI optimal estimation scheme is also performed. It is shown that the D_0 "adjustment" from the combined PR-TMI scheme is in the "correct" direction assuming the KPOL derived D_0 is assumed to be the ground truth. In essence, the method of retrieving D_0 from Kozu et al (2009) overestimated on average the KPOL-derived D_0 by 15-25% (normalized bias), whereas the combined PR-TMI method was able to reduce the normalized bias to -0.8% in one case and to <10% in the second case. This is a robust result pointing to the advantage of using the additional information provided by the TMI radiances in the retrieval of D_0. The variation of D_0 versus R from KPOL, 2A25 and combined PR-TMI (on which are superimposed contours of constant ε) are examined (see Fig. 10) for the two events. For rain rates between 10 and 30 mm h^{-1}, the D_0 values from the combined PR-TMI and KPOL tended, on average, towards larger ε as compared with the 2A25, more so in one event than the other. In essence, the D_0 statistics point to lower values than implied by the 2A25 algorithm for a given rain rate, or in other words the multiplicative coefficient 'a' in the $Z=aR^b$ is lower compared to 2A25. Both the 2A25 and the PR-TMI generally underestimated the KPOL-derived rain rates for R>25 mm h^{-1}. This underestimation is consistent with a systematic underestimate in the attenuation-corrected reflectivity from the 2A25 (for Z_e>40 dBZ) relative to KPOL-measured reflectivity (an explanation requiring a systematic offset to the KPOL calibration of 1.5-2.5 dB was determined to be unreasonable). The underestimation of 2A25 attenuation-corrrected Z_e could be related to the estimation of the PIA using the SRT methodology and the vertical structure model inherent to the 2A25. Obviously, data from two overpasses or "scenes" are not sufficient to draw more general conclusions, but case studies like the ones conducted herein should be extended to other rain regimes and over longer time periods.

Acknowledgements: VNB and GJH were supported by the NASA PMM Science grant NNX10AG74G. Development and use of the MK algorithm was supported by NASA Headquarters through the NASA Earth and Space Science Fellowship Program under Dr. Ming-Ying Wei and the Global Precipitation Science Program under Dr. Ramesh Kakar. DBW and DAM were supported by Drs. Arthur Hou and Matt Schwaller (TRMM Ground Validation) under NASA grant NNG06HX18C.

REFERENCES

Amemiya, Y., 1997: Generalization of the TLS approach in the errors-in-variables problem. *Recent Advances in Total Least Squares Techniques and Errors-in-Variables Modeling*, S. Van Huffel, Ed., SIAM, 77–86.

Awaka, J., T. Iguchi, and K. Okamoto, 2007: On rain type classification algorithm TRMM PR 2A23 V6. *Measuring Precipitation from Space: EURAINSAT and the Future.* Springer, New York, 213-224.

Beard, K. V. and R. J. Kubesh, 1991: Laboratory Measurements of Small Raindrop Distortion. Part 2: Oscillation Frequencies and Modes. *J. Atmos. Sci.*, **48**, 2245-2264.

Bolen, S. M. and V. Chandrasekar, 2003: Methodology for Aligning and Comparing Spaceborne Radar and Ground-Based Radar Observations. *J. Atmos. Oceanic Technol.*, **20**, 647-659.

Bowman, K. P., 2005: Comparison of TRMM Precipitation Retrievals with Rain Gauge Data from Ocean Buoys. *J. Climate.*, **18**, 178-190.

Brandes, E. A., G. Zhang and J. Vivekanandan, 2004: Drop Size Distribution Retrieval with Polarimetric Radar: Model and Application. *J. Appl. Meteor.*, **43**, 461-475.

Bringi, V. N. and V. Chandrasekar: 2001: *Polarimetric Doppler Weather Radar: Principles and Applications*, Cambridge University Press, 636.

Bringi, V. N., V. Chandrasekar, J. Hubbert, E. Gorgucci, W. L. Randeu and M. Schöenhuber, 2003: Raindrop Size Distribution in Different Climatic Regimes from Disdrometer and Dual-Polarized Radar Analysis. *J. Atmos. Sci.*, **60**, 354-365.

Bringi, V. N., C. R. Williams, M. Thurai, and P. T. May, 2009: Using dual-polarized radar and dual-frequency profiler for DSD characterization: a case study from Darwin, Australia. *J. Atmos. Oceanic Technol.*, **26,** 2107-2122.

Chandrasekar, V., W. Li and B. Zafar, 2005: Estimation of the raindrop size distribution from space-borne radar observations. *IEEE Trans. Geosci. Remote Sens.*, **43**, 1078-1086.

Chandrasekar, V., V. N. Bringi, S. A. Rutledge, A. Hou, E. Smith, G. S. Jackson, E. Gorgucci and W. A. Petersen, 2008: Potential Role Of Dual- Polarization Radar in the Validation Of Satellite Precipitation Measurements: Rationale and Opportunities. *Bull. Amer. Meteor. Soc.*, **89**, 1127-1145.

Ciach, G. J. and Krajewski, W. F., 1999: On the estimation of radar rainfall error variance. *Adv. Water Res.*, **22**, 585-595.

DeMoss, J. D. and K. P. Bowman, 2007: Changes in TRMM Rainfall due to the Orbit Boost Estimated from Buoy Rain Gauge Data. *J. Atmos. Oceanic Technol.*, **24**, 1598-1607.

Ferreira, F., P. Amayenc, S. Oury and J. Testud, 2001: Study and Tests of Improved Rain Estimates from the TRMM Precipitation Radar. *J. Appl. Meteor.*, **40**, 1878-1899.

Gorgucci, E., V. Chandrasekar, V. N. Bringi and G. Scarchilli, 2002: Estimation of Raindrop Size Distribution Parameters from Polarimetric Radar Measurements. *J. Atmos. Sci.*, **59**, 2373-2384.

Grecu, M., W.S. Olson and E. N. Anagnostou, 2004: Retrieval of Precipitation Profiles from Multiresolution, Multifrequency Active and Passive Microwave Observations. *J. Appl. Meteor.*, **43**, 562-575.

Haddad, Z.S. E.A. Smith, C.D. Kummerow, T. Iguchi, M.R. Farrar, S. L. Durden, M. Alves and W. S. Olson, 1997: The TRMM 'Day-1' Radar/Radiometer Combined Rain-Profiling Algorithm. *J. Meteor. Soc. Japan*, **75**, 799-809

Hitschfeld, W. and J. Bordan, 1954: Errors inherent in the radar measurement of rainfall at attenuating wavelengths. *J. Meteor.*, **11**, 58-67.

Houze Jr, R. A., S. Brodzik, C. Schumacher, S. E. Yuter and C. R. Williams, 2004: Uncertainties in Oceanic Radar Rain Maps at Kwajalein and Implications for Satellite Validation. *J. Appl. Meteor.*, **43**, 1114-1132.

Hu, Z. and R. C. Srivastava, 1995: Evolution of Raindrop Size Distribution by Coalescence, Breakup, and Evaporation: Theory and Observations. *J. Atmos. Sci.*, **52**, 1761-1783.

Huang, G., V. N. Bringi and M. Thurai, 2008: Orientation angle distributions of drops after 80 m fall using a 2D video disdrometer. *J. Atmos. Oceanic Technol.*, **25**, 1717--1723.

Hubbert, J. and V. N. Bringi, 1995: An Iterative Filtering Technique for the Analysis of Copolar Differential Phase and Dual-Frequency Radar Measurements. *J. Atmos. Ocean Tech.*, **12** , 643-648.

Iguchi, T., T. Kozu, R. Meneghini, J. Awaka and K. Okamoto, 2000: Rain-Profiling Algorithm for the TRMM Precipitation Radar. *J. Appl. Meteor.*, **39**, 2038-2052.

Iguchi, T., T. Kozu, J. Kwiatkowski, R. Meneghini, J. Awaka and K. Okamoto, 2009: Uncertainties in the rain profiling algorithm for the TRMM precipitation radar. *J. Meteor. Soc. Japan*, **87A**, 53-66.

Illingworth, A. J. and T. Mark Blackman, 2002: The Need to Represent Raindrop Size Spectra as Normalized Gamma Distributions for the Interpretation of Polarization Radar Observations. *J. Appl. Meteor.*, **41**, 286-297.

Joss, J. and A. Waldvogel, 1967: A raindrop spectrograph with automatic analysis. *Pure Appl. Geophys.*, **68**, 240-246.

Kozu, T., T. Iguchi, T. Kubota, N. Oshida, S. Seto, J. Kwiatkowski and Y. Takayabu, 2009: Feasibility of raindrop size distribution parameter estimation with TRMM precipitation radar. *J. Meteor. Soc. Japan*, **87A**, 53-66.

Lee, G. W. and I. Zawadzki, 2005: Variability of Drop Size Distributions: Noise and Noise Filtering in Disdrometric Data. *J. Appl. Meteor.*, **44**, 634-652.

Liu, Y., V. N. Bringi and T. D. Keenan, 2003: Comparisons of raindrop size distributions from the TRMM precipitation radar and the C-POL ground radar. *31st Int. Conf. Radar Meteor.*, American Met. Soc., Seattle, Washington, **2**, 429-432.

Marks, D. A., D. B. Wolff, D. S. Silberstein, A. Tokay, J. L. Pippitt and J. Wang, 2009: Availability of High-Quality TRMM Ground Validation Data from Kwajalein, RMI: A Practical Application of the Relative Calibration Adjustment Technique. J. *Atmos. Oceanic Technol.*, **26**, 413-429.

Marks, D. A., D. B. Wolff, L. D. Carey and A. Tokay, 2011: Quality Control and Calibration of the Dual-Polarization Radar at Kwajalein, RMI. *J. Atmos. Oceanic Technol.*, **28**, 181-196.

Meneghini, R. and J. A. Jones, 2011: Standard Deviation of Spatially Averaged Surface Cross

Section Data from the TRMM Precipitation Radar. *IEEE Geosci. and Rem. Sens. Lett.*, **8**, 293-297

Munchak, S.J. and C. D. Kummerow, 2011: A modular optimal estimation method for combined radar-radiometer precipitation profiling. *J. Appl. Meteor. Climatol.*, **50**, 433-448.

Ryzhkov, A. V., S. E. Giangrande and T. J. Schuur, 2005: Rainfall Estimation with a Polarimetric Prototype of WSR-88D. *J. Appl. Meteor.*, **44**, 502-515.

Schumacher, C. and R. A. Houze Jr., 2000: Comparison of Radar Data from the TRMM Satellite and Kwajalein Oceanic Validation Site. *J. Appl. Meteor.*, **39**, 2151-2164.

Schwaller, M. R. and K. Robert Morris, 2011: A Ground Validation Network for the Global Precipitation Measurement Mission. *J. Atmos. Oceanic Technol.*, **28**, 301-319.

Sheppard, B. E., and P. I. Joe, 1994: Comparison of raindrop size distribution measurements by a Joss-Waldvogel disdrometer, a PMS 2DG spectrometer, and a POSS Doppler radar. *J. Atmos. Oceanic Technol.*, **11**, 874-887.

Silberstein, D. S., D. B. Wolff, D. A. Marks, D. Atlas and J. L. Pippitt, 2008: Ground Clutter as a Monitor of Radar Stability at Kwajalein, RMI. *J. Atmos. Oceanic Technol.*, **25**, 2037-2045.

Steiner, M., J. A. Smith and R. Uijlenhoet, 2004: A Microphysical Interpretation of Radar Reflectivity–Rain Rate Relationships. *J. Atmos. Sci.*, **61**, 1114-1131.

Stephens, G. L. and C. D. Kummerow, 2007: The Remote Sensing of Clouds and Precipitation from Space: A Review. *J. Atmos. Sci.*, **64**, 3742-3765

Testud, J., S. Oury, R. A. Black, P. Amayenc, and X. Dou, 2001: The concept of “Normalized” distribution to describe raindrop spectra: A tool for cloud physics and cloud remote sensing. *J. Appl. Meteorol.*, **40**, 1118-1140.

Thurai, M., G. Huang, V. N. Bringi, W. L. Randeu, and M. Schönhuber, 2007: Drop shapes, model comparisons, and calculations of polarimetric radar parameters in rain. *J. Atmos. Oceanic Technol.*, **24**, 1019-1032.

Thurai, M., V. N. Bringi and P. T. May, 2010: CPOL Radar-Derived Drop Size Distribution Statistics of Stratiform and Convective Rain for Two Regimes in Darwin, Australia. *J. Atmos. Oceanic Technol.*, **27**, 932-942.

Tokay, A. and D. A. Short, 1996: Evidence from Tropical Raindrop Spectra of the Origin of Rain from Stratiform versus Convective Clouds. *J. Appl. Meteor.*, **35**, 355-371.

Trenberth, K. E., J. T. Fasullo and J. Kiehl, 2009: Earth's Global Energy Budget, *Bull. Amer. Meteor. Soc.* **90**, 311-323.

Ulbrich, C. W. and D. Atlas, 1998: Rainfall Microphysics and Radar Properties: Analysis Methods for Drop Size Spectra. *J. Appl. Meteor.*, **37**, 912-923.

Wang, J., and D. B. Wolff, 2009: Comparisons of reflectivities from the TRMM Precipitation Radar and ground-based radars. *J. Atmos. Oceanic Technol.*, **26**, 857–875.

Williams, C. R., A. Kruger, K. S. Gage, A. Tokay, R. Cifelli, W. F . Krajewski, and C. Kummerow, 2000: Comparison of simultaneous rain drop size distributions estimated from two surface disdrometers and a UHF profiler. *Geophys. Res. Lett.*, **27**, 1763-1766.

Wolff, D. B., D. A. Marks, E. Amitai, D. S. Silberstein, B. L. Fisher, A. Tokay, J. Wang and J. L. Pippitt, 2005: Ground Validation for the Tropical Rainfall Measuring Mission (TRMM). *J. Atmos. Oceanic Technol.*, **22**, 365-380.

Wolff, D. B and B. L. Fisher, 2008: Comparisons of Instantaneous TRMM Ground Validation and Satellite Rain-Rate Estimates at Different Spatial Scales. *J. Appl. Meteor. Climatol*., **47**, 2215-2237.